Percolation phenomena in disordered topological networks

V. Rodriguez[♯], **Y. Diao** [†] **and J. Arsuaga**[*,‡]

[♯]Department of Physics and Astronomy
San Francisco State University
San Francisco, CA 94116
[†]Department of Mathematics and Statistics
University of North Carolina at Charlotte
Charlotte, NC 28223
[*]Department of Mathematics
San Francisco State University
San Francisco, CA 94116
[‡] To whom correspondence should be addressed

Abstract. Topological polymer networks are networks made of circular polymers that are topologically linked. Topological networks made of small circular DNA or protein molecules are of great interest in biology and nanotechnology because they are found in living organisms and can be constructed in-vitro. The physical factors that determine the topology of a network as well as the pathways that are followed for its formation remain poorly understood. In our previous work we proposed a novel biophysical/computational approach to model the formation of planar DNA minicircle networks in trypanosomatid parasites. This model suggests that minicircle networks in trypanosomatid parasites emerged from topologically free minicircles upon space confinement through a percolation pathway. This model however is somewhat idealized because it assumes that the centers of the minicircles in the network are regularly positioned across a planar lattice. Here we propose an extension of the model by allowing the centers of the minicircles to be randomly placed in a planar surface. We numerically show that upon increasing minicircle density, networks form, following a percolation pathway. Our model suggests that the critical percolation density increases as $D^{perc} = 0.8357 - 1.4297\exp(0.6439x)$ with x is the maximum displacement. Our results therefore show that minicircle positioning does not dramatically affect the process of network formation through percolation supporting therefore that networks made of circular polymers may follow this pathway during their formation.

1. Introduction

Topological polymer networks are networks that are held together through topological interactions of their subunits. Traditionally, topological polymer networks have been studied in the context of olympic gels where short linear polymers are cyclized in the presence of minicircles [14, 15, 17]. However topological networks are also found in diverse biological systems such as the protein network that makes up the capsid of bacteriophage HK97 [11, 20] or the DNA network found in the mitochondrion of trypanosomatid parasites (reviewed in [18]). In vitro assays also can produce complex topological networks as in the case of type II topoisomerases assays [13] and of DNA nanotechnology assays (e.g. [14]).

Theoretical studies of topological networks were pioneered by de Gennes [15]. More recently, and motivated by DNA networks found in the kinetoplast of trypanosomatids [9], parasitic organisms that cause fatal diseases in human and livestock, we have proposed a new theoretical approach to study the formation of topological networks. Our model relies in several features that are only found in the networks of Trypanosomatid parasites. First, they are made of small DNA molecules ($\leq$ 2.5kb) and their centers are placed on a plane (hence the name planar network) [12]. Second, any two minicircles are topologically linked by a single interlock [16]. Third the number of minicircles linked to any given minicircle is cell cycle dependent and the value is either three or six [3, 4].

In [9] we proposed that space confinement (or high density) of DNA minicircles is a key factor in the formation of minicircle networks in these organisms. To test this hypothesis we introduced a model in which randomly oriented, geometric minicircles are placed on the vertices of a square lattice. Our results showed that increasing density of minicircles triggers the formation of percolating clusters, defined as clusters of topologically linked minicircles that span the length of the lattice. This model however may be an oversimplification of the network found in trypanosomatid parasites since for instance, the density at which percolation occurs depends on the specific lattice employed [7]. We here consider a model in which the placement of the minicircles have some degree of randomness deviating it from the lattice model. We find that a percolation pathway is a rather robust phenomena that is observed upon minicircle confinement.

2. Methods

2.1. Lattice generation and minicircle placement

Two dimensional square lattice models were generated as described in [9]. In brief, the center of each minicircle was placed at a unique lattice point and no two minicircles shared the same center; the orientation of each minicircle was determined by its normal vector which was sampled uniformly over the unit sphere. Disordered (irregular) lattices were generated by displacing each lattice point uniformly over a disc centered at the lattice vertex with radius given by a predetermined maximum displacement (M_{disp}), measured in terms of the distance between two adjacent lattice points. Similarly to the model of [9], the density of minicircles in this model is defined by the number of minicircles per unit area where the radius of the minicircles is used as the unit length. Consequently, if the distance between two adjacent lattice points in the square lattice is r, then the density of minicircles of the model is given by $1/r^2$.

2.2. Topological linking between minicircles

Let C_1 and C_2 be two disjoint minicircles in $\mathbb{R}^3$ (namely two circles that do not intersect each other). We say that C_1 and C_2 form an unsplittable link/non-trivial topological link (of two components) if no topological 2-sphere separates them. The same definition can be extended to the general case where there are n disjoint simple closed curves in $\mathbb{R}^3$. To determine whether two minicircles were linked we used a geometrical criterion that we introduced in [9]. Given two minicircles C_1 and C_2 of fixed radius r centered at P and Q respectively, consider the planes that contain the minicircles, together with the plane that bisects P and Q (so that it goes through the midpoint O of P and Q and is perpendicular to the line segment PQ). With probability one, these three planes intersect at a single point x. As illustrated by Figure 1, C_1 and C_2 form an unsplittable link if and only if $R > |Px| = |Qx|$. This method is faster than other methods that help determine whether two curves form a non-trivial link or not but it is only applicable to geometric minicircles.

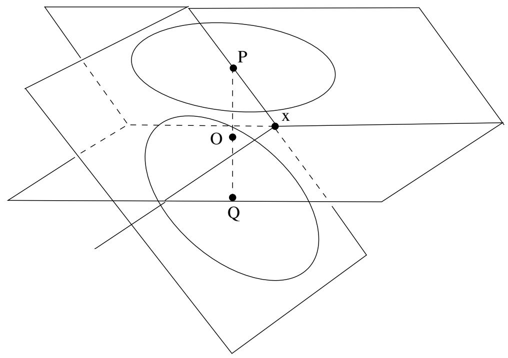

Figure 1. The relative positions of two minicircles and the bisecting plane of their centers. In the shown case the radius of the minicircles is less than $|Px| = |Qx|$ and they are clearly unlinked.

2.3. An approach to the estimation of the percolation density in disordered topological networks

In order to determine the growth properties of minicircle networks we represent each minicircle as a point and the linking between two minicircles as a bond between two points. In our previous studies we have determined percolation based on the existence of clusters that could span the length the lattice. Disordered lattices do not have well defined lattice edges therefore these methods are not suitable. To calculate the critical percolation probabilities on two-dimensional random point distributions we extended the methods developed by Becker and Ziff [2]. In their work, randomized lattices with periodic boundary conditions were first generated using partitions of the plane. Clusters were grown from randomly selected points (called seed points) by connecting nearby points to the cluster according to a preselected probability p. This process was iterated until no more bonds could be formed or a pre-determined cluster size cut-off limit was reached. Percolation was determined by the distribution of cluster sizes as discussed next.

Let P_s be the probability that a cluster grew to be at least size s and p_c be the critical percolation probability. Then we may assume that P_s grows as $As^{2-\tau}f[B(p-p_c)s^{\sigma}]$ where $\tau = 187/91$ is the Fisher exponent for the two-dimensional percolation cluster universality class, $\sigma = 63/91$ and f is a the universal scaling function which measures the probability of occurrence of large clusters. By computing the Taylor expansion of f near the p_c we obtain $P_s \sim s^{2-\tau}[A+D(p-p_c)s^{\sigma}+...]$ and if we define $C_s = P_s s^{\tau-2}$ then $C_s \sim [A+D(p-p_c)s^{\sigma}]$ which means that for large values of s C_s grows linearly with s^{σ} and its slope vanishes when p is equal to the critical percolation probability.

By substituting D_c, the critical minicircle density, for p_c we are then able to adapt Becker and Ziff's method to estimate the critical percolation density for disordered minicircle networks.

3. Results

3.1. Estimation of Fisher exponent τ_{mini} in minicircle networks

The Becker-Ziff method was developed to estimate the critical percolation probability for site and bond percolation on random lattices. To test that our model is consistent with these models and therefore the methods proposed by Becker-Ziff can be used in our minicircle model we first aimed at determining whether minicircle clusters grow in accordance with the critical exponents assumed in the Becker-Ziff method. For this reason we estimated the value of the Fisher exponent τ by studying the size distribution of minicircle clusters grown on the regular square lattice.We denote the estimated value τ_{mini}.

In independent bond and site percolation problems, n_s, the number of clusters of size s per lattice site, obeys the general scaling relation $n_s(p) = s^{-\tau} f[(p - p_c)s^{\sigma}]$, where the behavior of the scaling function f can be approximated numerically [19]. As $p \to p_c$, f approaches a constant value. Thus, for $p \sim p_c$, $n_s(p) \sim k \cdot s^{-\tau}$ for some positive constant k. Using this relation, τ_{mini} can then be approximated by the slope of the linear fit of a log-log plot of the observed cluster size distribution N_s ($N_s = n_s \times K^2$ where the lattice is of dimension $K \times K$) using the critical percolation density $D_c = 0.637$ [9]. Figure 2 shows our numerical results based on minicircle clusters generated on 1000×1000 regular square lattices with a sample of 1.2×10^7 minicircle clusters. The graph shows the linear regression fit to the log of the cluster size s and the number of clusters of that size N_s. Our estimated value for τ_{mini} is 2.02 ± 0.06, which is in agreement with the value of τ for the 2-dimensional percolation cluster universality class. From this result we conclude that the methods developed in [2] are amenable for our study.

3.2. Estimation of the critical percolation density in the square lattice

To validate our approach, we first estimated the square lattice critical percolation density and compared with the value of $D_c \sim 0.637$ obtained in [9]. As described in Subsection 2.3 we expect that for large clusters the slope of C_s is a constant and that at $D = D_c$ the slope of $C_s = 0$. We then first estimated C_s as a function of s^{σ}.

Figure 3 shows our numerical results. Notice that each curve in the figure shows the value of C_s for a different density values near 0.637. As expected the slope of each curve is constant for large clusters and by mere inspection one can appreciate that the value closest to the known percolation density seems to have zero slope.

To confirm this observation we proceeded as in [2]. We computed the slope of the best linear fit to each curve C_s for $s^{\sigma} \geq 10$. Since the value at which percolation occurs (i.e. slope of $C_s = 0$) may be in between any two of the tested density values, the best linear fit relating the growth of the slope of C_s with respect to the density and the x-intercept of the best fit was computed. Figure 4 (bottom) displays the best linear fit and the x-intercept highlighted. Our estimated value for $D_{perc} = 0.6370$ which is in exact agreement with the critical percolation density obtained in [9].

In order to test the dependence of our results on the s^{σ} value used on our linear fit we repeated the study with the linear fits for C_s for large s^{σ} for the cases $s^{\sigma} \geq 9.5$, $s^{\sigma} \geq 10$, $s^{\sigma} \geq 10.5$ and $s^{\sigma} \geq 11$. Our results are shown in the following table. The data in the table shows that when we restrict the fitting range to larger s^{σ} values, the

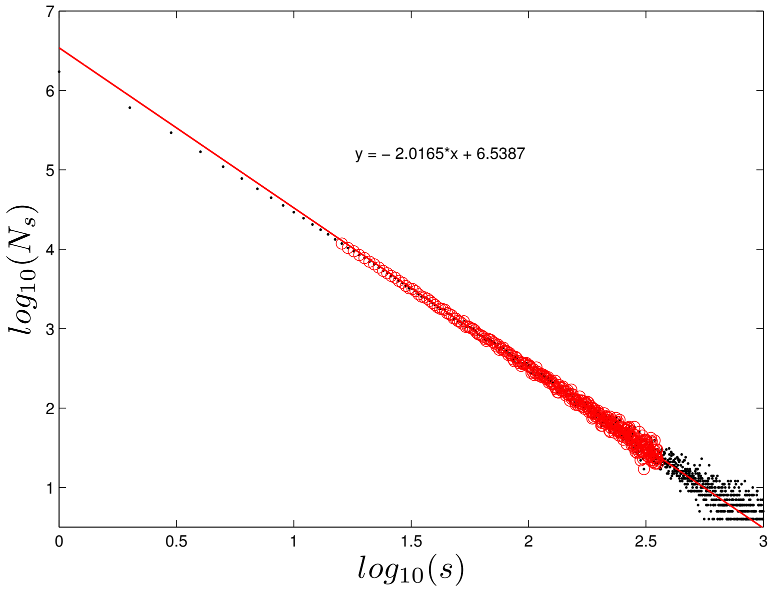

Figure 2. Log-log plot of N_s vs. s. The linear regression fit to $\log(N_s)$ vs. $\log(s)$ yields a τ_{mini} value which approximates the accepted traditional site and bond percolation $\tau = 187/91 \approx 2.055$ within one standard deviation.

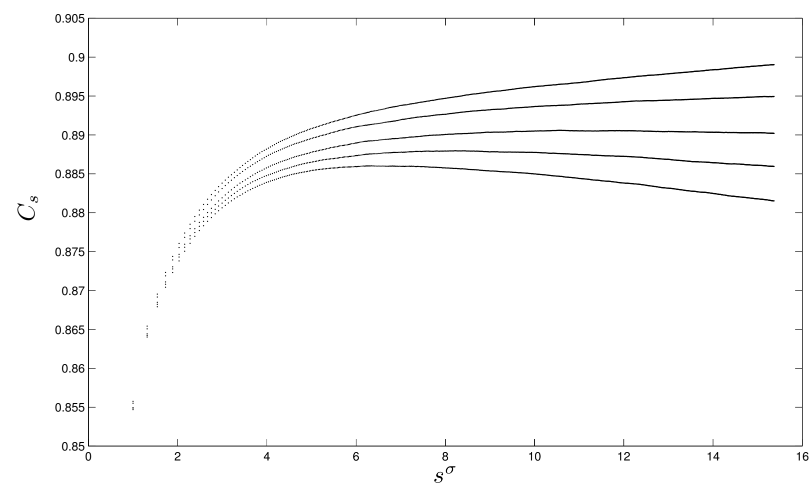

Figure 3. C_s curves for minicircle clusters grown for $D = 0.6363$, 0.6366, 0.6370, 0.6373, 0.6376 from bottom to top. The sample size is 10^7 for each density value.

changes in the slopes of C_s vs. s^σ regression lines are quite small: they are all in the fifth order for each density tested.

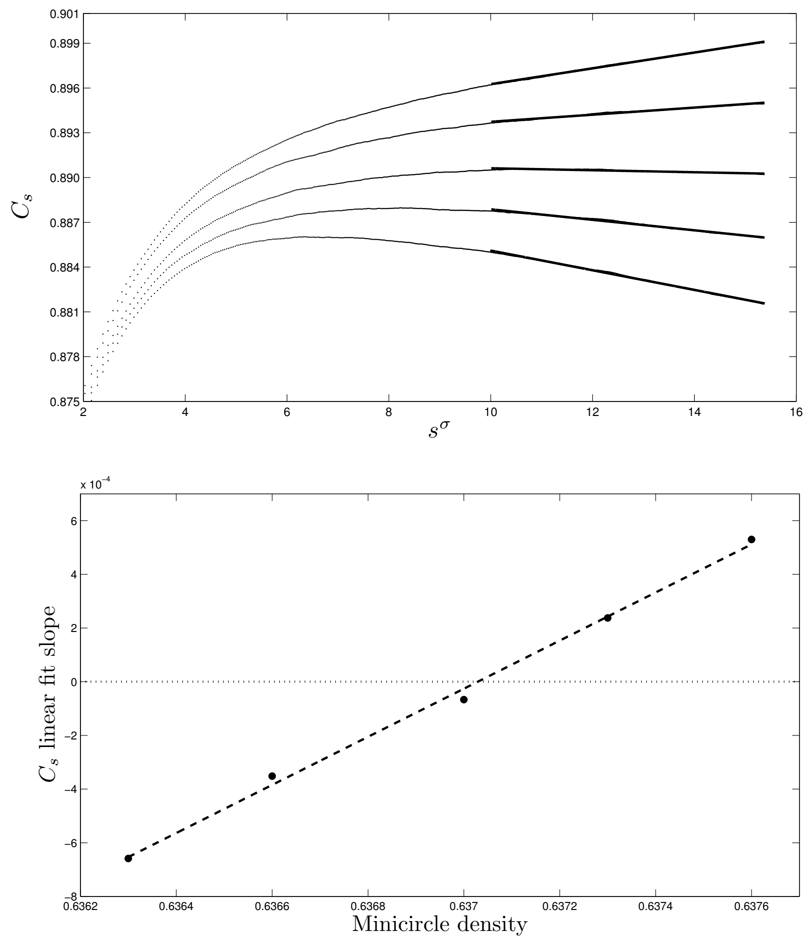

Figure 4. *Top:* Linear relationship between C_s and s^σ for large s in the regular square lattice. Curves were generated using 10^7 independent clusters grown at minicircle densities of $D = 0.6363, 0.6366, 0.6370, 0.6373, 0.6376$. Best fit lines for $s^\sigma \geq 10$ are shown to highlight the near linear behavior of C_s for large values of s^σ. *Bottom:* The linear regression line of the corresponding slopes of C_s best-fit lines from the top figure ($y = 0.89598x - 0.57077$, $R^2 = 0.9992$). The best fit line intersects the horizontal line at a minicircle density of 0.63703.

3.3. Estimation of the percolation density in disordered lattices

Our previous results validate our approach and next we aim to employ these methods to determine the critical percolation densities in disordered lattices. We generated disordered lattices as described in the methods section with maximum displacement magnitudes of 0.5, 1.0, 1.5, 2.0, 2.5 and 3.0. Figure 5 shows examples of two disordered lattices with different maximum displacements and same minicircle density. The figure highlights the different clusters.

minicircle density	min. s^σ	slope of lin. fit $\cdot 10^{-4}$
0.6363	9.5	-6.4851
	10.0	-6.5843
	10.5	-6.6722
	11.0	-6.7593
0.6366	9.5	-3.4024
	10.0	-3.5171
	10.5	-3.6150
	11.0	-3.7172
0.6370	9.5	-0.5547
	10.0	-0.6666
	10.5	-0.7397
	11.0	-0.7824
0.6373	9.5	2.4597
	10.0	2.3775
	10.5	2.3046
	11.0	2.2004
0.6376	9.5	5.3423
	10.0	5.2980
	10.5	5.2518
	11.0	5.1642

Table 1. C_s linear slope dependence on s^σ range.

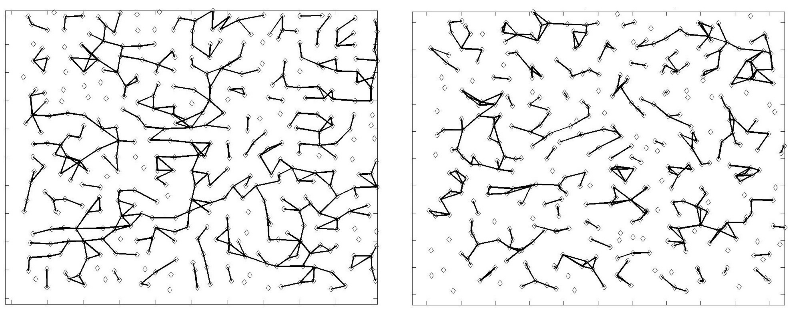

Figure 5. Minicircle clusters in disordered lattices with maximum displacement of 0.5 (left) and 1.0 (right) and density of 0.64.

As in the previous section the growth of C_s was calculated and linearly approximated for $s^\sigma \geq 10$ (similar results would be obtained if a different range of s^σ were used, so long as it is large enough, as indicated by Table 1). The results are shown in Figures 6 to 11 for the cases of maximum displacements 0.5, 1.0, 1.5, 2.0, 2.5 and 3.0. These results are consistent with those obtained in the previous section and across disordered lattices. A visual inspection of these results already reveals that C_s tends to be noisier for larger displacements and that the percolation density grows with the displacement. The growth of the percolation density is clearly appreciated in the overall range of the slopes of the linear approximations of C_s.

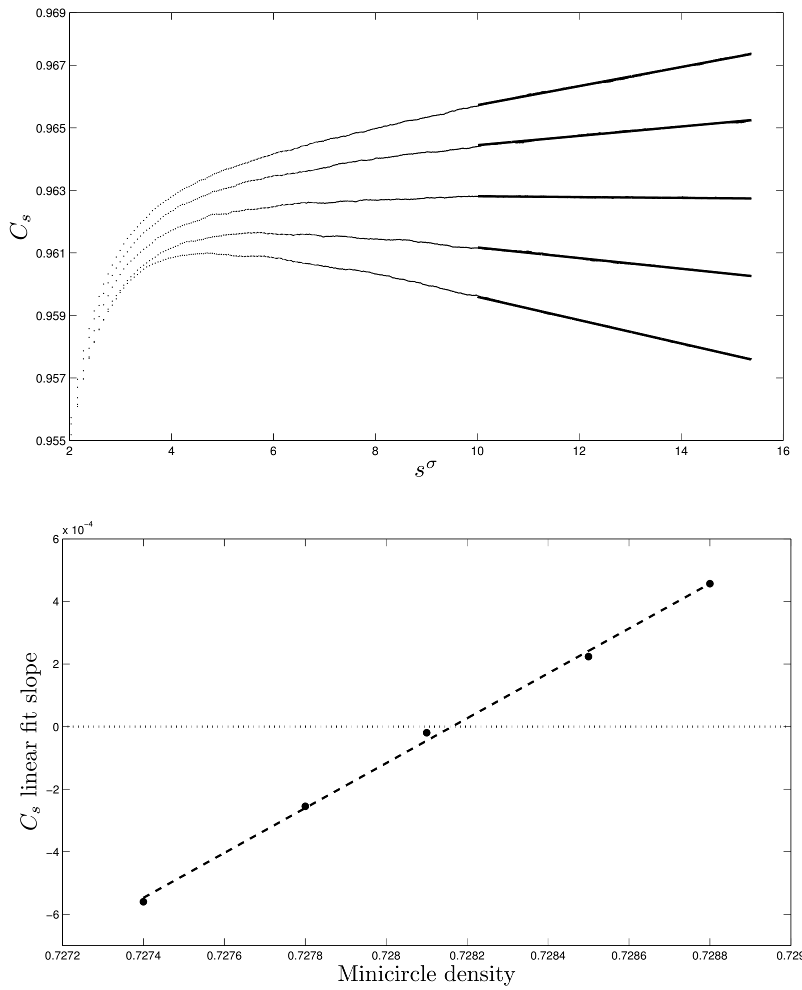

Figure 6. *Top:* C_s curves for lattices of maximum displacement 0.5 evaluated at minicircle densities 0.7274, 0.7278, 0.7281, 0.7285 and 0.7288 (from bottom to top). 5×10^6 clusters were sampled for each curve. *Bottom:* The linear regression line of the corresponding slopes of C_s best-fit lines ($y = 0.71742x - 0.52240$, $R^2 = 0.9995$). The best fit line intersects the horizontal line at a minicircle density of 0.72816.

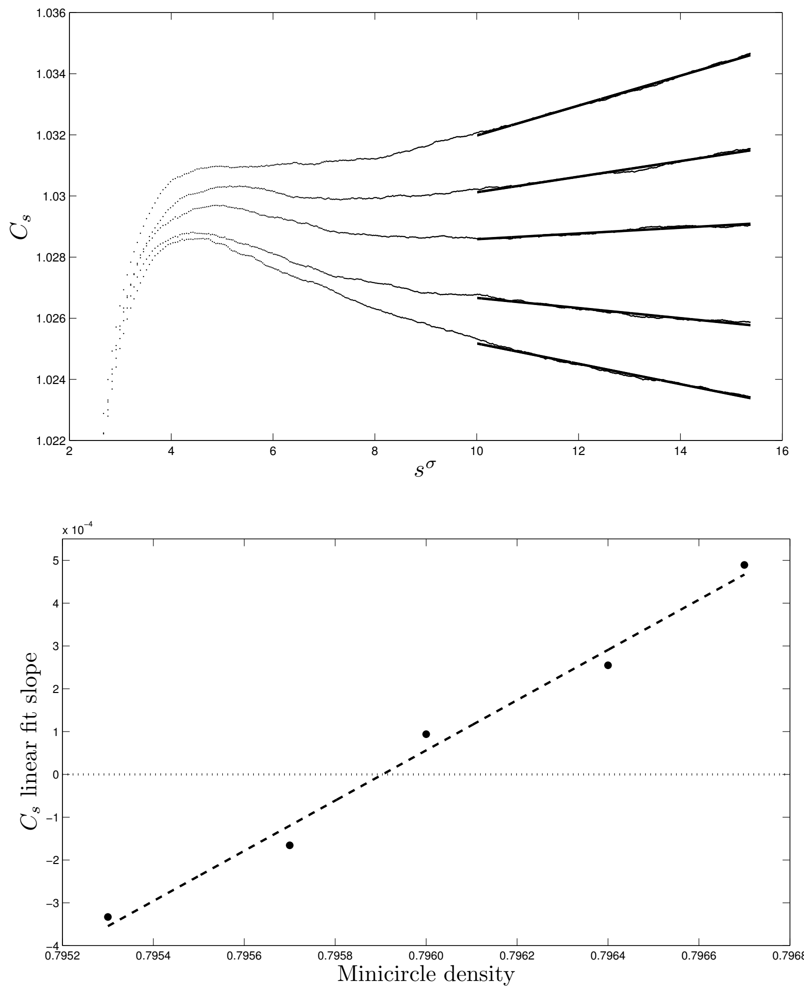

Figure 7. *Top:* C_s curves for lattices of maximum displacement 1.0 evaluated at minicircle densities 0.7953, 0.7957, 0.7960, 0.7964 and 0.7967 (from bottom to top). 5×10^6 clusters were sampled for each curve. *Bottom:* The linear regression line of the corresponding slopes of C_s best-fit lines ($y = 0.58672x - 0.46697$, $R^2 = 0.9948$). The best fit line intersects the horizontal line at a minicircle density of 0.79590.

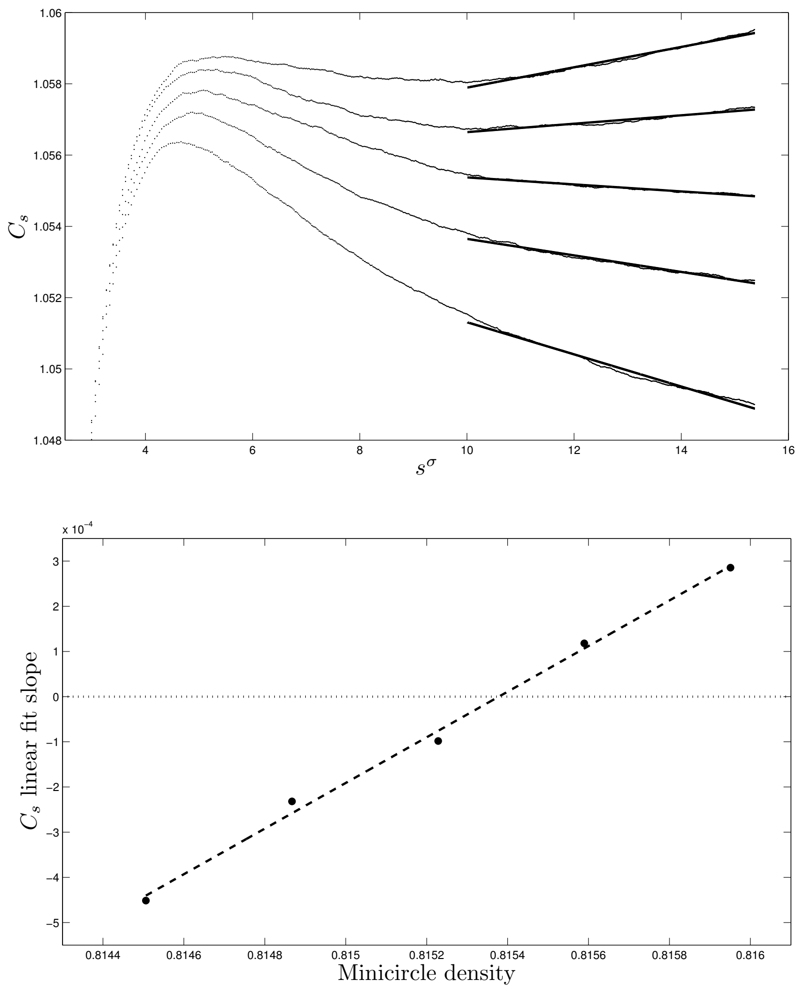

Figure 8. *Top:* C_s curves for lattices of maximum displacement 1.5 evaluated at minicircle densities 0.8145, 0.8149, 0.8152, 0.8156 and 0.8160 (from bottom to top). 5×10^6 clusters were sampled for each curve. *Bottom:* The linear regression line of the corresponding slopes of C_s best-fit lines ($y = 0.50491x - 0.41170$, $R^2 = 0.9990$). The best fit line intersects the horizontal line at a minicircle density of 0.81537.

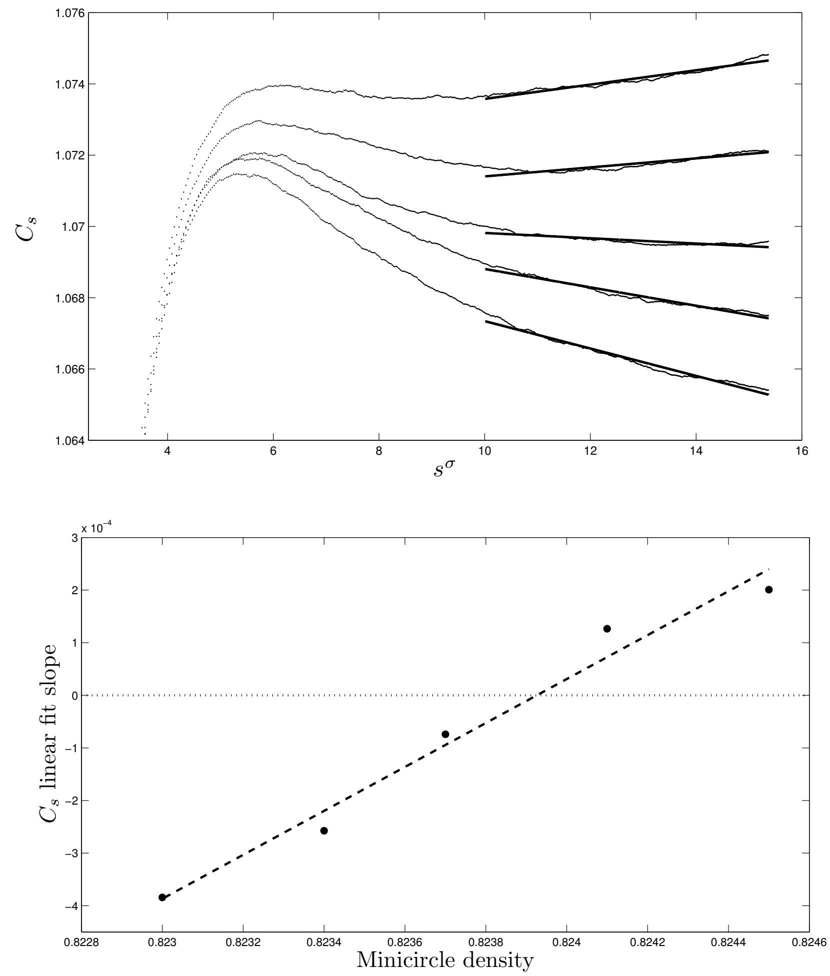

Figure 9. *Top:* C_s curves for lattices of maximum displacement 2.0 evaluated at minicircle densities 0.8230, 0.8234, 0.8237, 0.8241 and 0.8245 (from bottom to top). 5×10^6 clusters were sampled for each curve. *Bottom:* The linear regression line of the corresponding slopes of C_s best-fit lines ($y = 0.41766x - 0.34412$, $R^2 = 0.9839$). The best fit line intersects the horizontal line at a minicircle density of 0.82393.

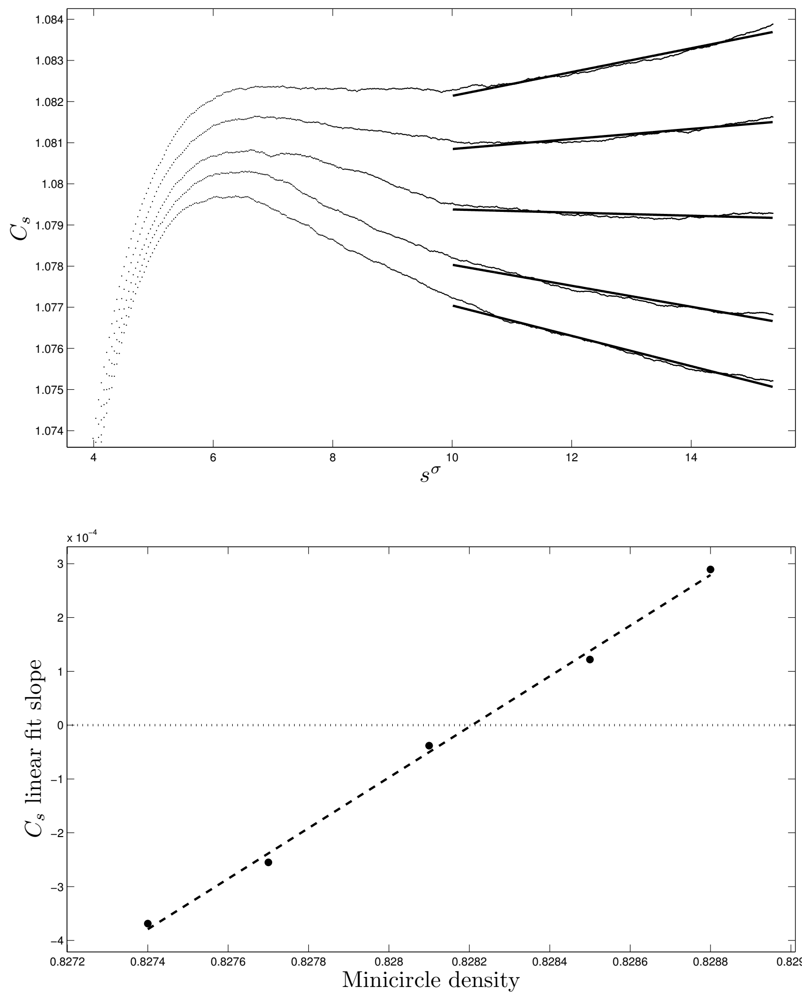

Figure 10. *Top:* C_s curves for lattices of maximum displacement 2.5 evaluated at minicircle densities 0.8274, 0.8277, 0.8281, 0.8285 and 0.8288 (from bottom to top). 5×10^6 clusters were sampled for each curve. *Bottom:* The linear regression line of the corresponding slopes of C_s best-fit lines ($y = 0.47026x - 0.38947$, $R^2 = 0.9983$). The best fit line intersects the horizontal line at a minicircle density of 0.82821.

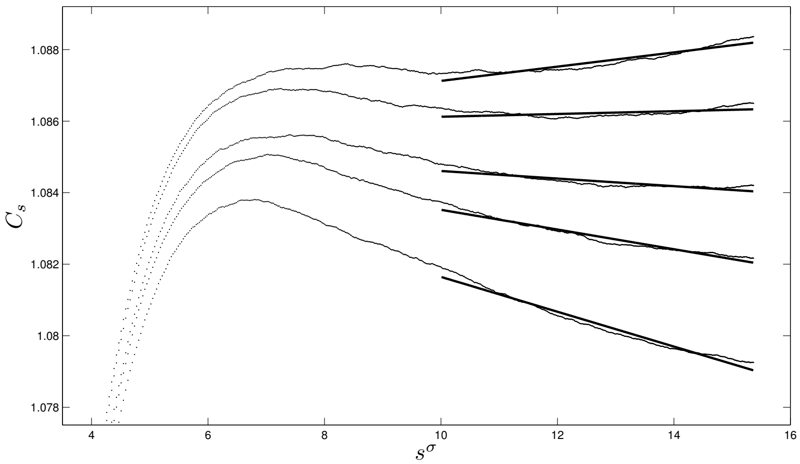

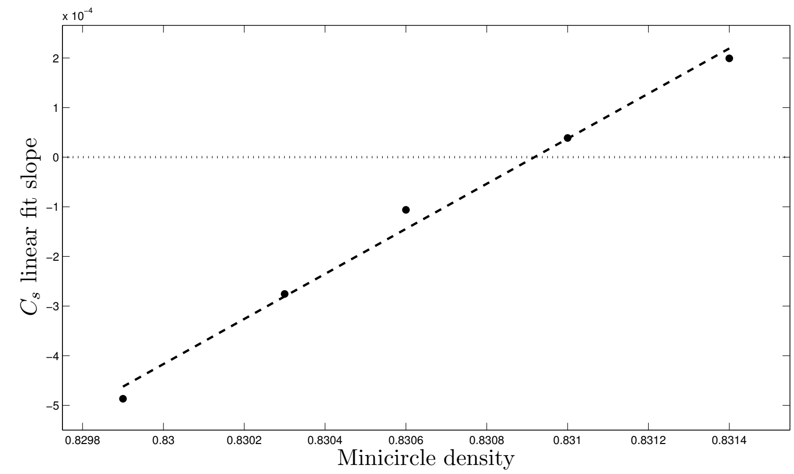

Figure 11. *Top:* C_s curves for lattices of maximum displacement 3.0 evaluated at minicircle densities 0.8299, 0.8303, 0.8306, 0.8310 and 0.8314 (from bottom to top). 5×10^6 clusters were sampled for each curve. *Bottom:* The linear regression line of the corresponding slopes of C_s best-fit lines ($y = 0.45449x - 0.37764$, $R^2 = 0.9958$). The best fit line intersects the horizontal line at a minicircle density of 0.83092.

Notice that while the minicircle densities sampled for the square lattice without displacement range from 0.6363 to 0.6376, those corresponding for a maximum displacement of 0.5 range from 0.7274 to 0.7288 and those corresponding to a maximum displacement of 3.0 range from 0.8299 to 0.8314. The critical percolation density for each disordered lattice is estimated using a linear approximation of the growth of the slopes as a function of minicircle density as shown in the right panels of figures 6 to 11. The estimated critical percolation densities are 0.7282 for $M_{disp} = 0.5$, 0.7959 for $M_{disp} = 1.0$, 0.8154 for $M_{disp} = 1.5$, 0.8239 for $M_{disp} = 2.0$, 0.8282 for $M_{disp} = 2.5$ and 0.8309 for $M_{disp} = 3.0$. Next we characterized the growth of the critical percolation density as a function of the maximum displacement. Results are shown in Figure 12 where the critical percolation densities are plotted against the maximum displacements. These results seem to suggest that the critical percolation density will level off as the maximum displacement increases. The fitted curve in Figure 12 has the form $y = a - b\exp(-cx)$ where a, b and c are real-valued constants. As x grows large, y approaches $a = 0.83579$, which is our estimate of the limiting value for the critical percolation density as a function of maximum displacement.

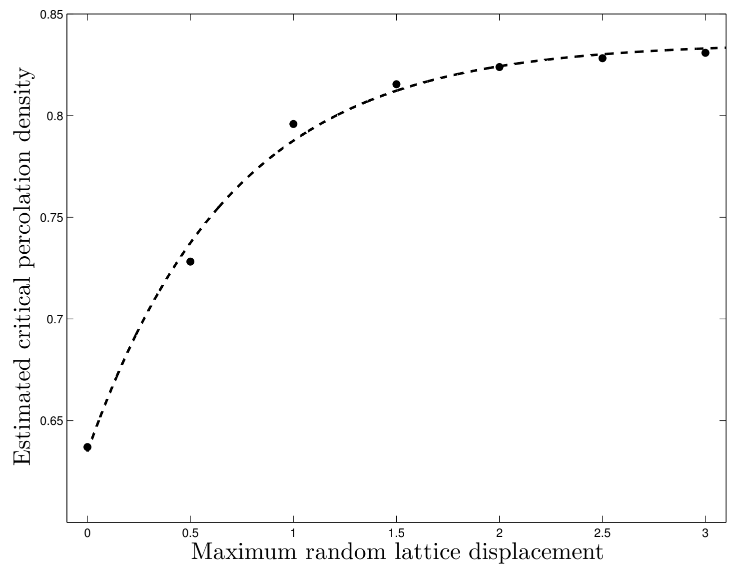

Figure 12. Percolation densities for maximum randomization magnitudes between 0.0 and 3.0. The critical percolation density increases monotonically as the maximum displacement magnitude is increased. The equation of the fitted curve is $y = 0.83579 - 1.42980e^{-0.64392x}$ ($R^2 = 0.9944$).

4. Conclusions

Topological networks made of small minicircles are important in the engineering of olympic gels and of new materials [14, 15, 17] and in the formation of biologically relevant structures [11, 13, 18, 20]. In [9] we introduced a new theoretical model to study the formation of DNA minicircle networks in trypanosomatid parasites. Our model allowed us to characterize the effect of confinement [9], of the relative minicircle position[7], of the relative orientation of minicircles [1] and of DNA volume exclusion [8] in the formation of networks. All these models confirm the existence of a percolation pathway which suggest that the same pathway may be present in the formation of large topological networks in biological systems. The density at which percolation occurs depends on the parameters of the model. Interestingly our results showed that the relative orientation of the minicircles that has the most dramatic effect on percolation. All these studies however assume that minicircles are regularly positioned across a planar lattice. This assumption limits the applications of the model to structures that are crystalline like and even in those cases they still represent a somewhat idealized situation. In this study we have investigated the growth of networks on randomized lattices extending the methods developed by Becker and Ziff [2]. Our results show that disordered topological networks also show a percolation pathway when the density of minicircles is increased and that the critical percolation density increases as $D^{perc} = 0.8357 - 1.4297\exp(-0.6439x)$ with the maximum displacement of minicircles. These results therefore support our hypothesis that networks in trypanosomatid parasites grew through a percolation pathway and serve as a first step in the modeling of networks grown in more diluted conditions as those grown in-vitro in the presence of type II topoisomerases [13].

References

[1] Arsuaga, J., Diao, Y., Hinson, K. 2012 The effect of angle restriction on the topological characteristics of minicircle networks, *J. of Stat. Phys.*, **146**(2), 434–445

[2] Becker A.M. and Ziff R.M. (2009) Percolation thresholds on two-dimensional Voronoi networks and Delaunay triangulations, *Phys. Rev. E*

[3] Chen J., Rauch C.A., White J.H., Englund P.T., Cozzarelli N.R. 1995 The topology of the kinetoplast DNA network. *Cell* **80**(1) 61–69.

[4] Chen, J., Englund, P.T., Cozzarelli, N.R. Changes in network topology during the replication of kinetoplast DNA. 1995 *EMBO J.* **14**(24) 6339–6347.

[5] De Gennes PG 1979, *Scaling Concepts in Polymer Physics*, Cornel University Press.

[6] Diao, Y. 1994 Unsplittability of Random Links, *J. Knot Theor. Ramif.* **3**(3), 379–389.

[7] Diao Y, Hinson K, and Arsuaga J. 2012 The growth of minicircle networks on regular lattices, *J. Phys. A: Math. Theor.* **45** 035004

[8] Diao Y, Hinson K, and Arsuaga J. 2013 The effect of volume exclusion in the formation of minicircle networks *Submitted*.

[9] Diao Y., Hinson K., Kaplan R., Vazquez M. and Arsuaga J. 2012 The effects of minicircle density on the topological structure of the mitochondrial DNA from trypanosomes. *J. Math. Biol.*, **64**(6), 1087–1108.

[10] Diao Y., van Rensburg J. 1998 The Percolation of Linked Circles; , *Topology and Geometry in Polymer Science*, editors S. G. Whittington et al, the IMA Volumes in Mathematics and its Applications, **103**, 79–88.

[11] Duda RL 1998 Protein Chainmail: Catenated Protein in Viral Capsids.*Cell* **94**(1) 55–60

[12] Ferguson M., Torri A. F., Perez-Morga D., Ward D. C. and Englund P.T. 1992 In situ hybridization to the Crithidia fasciculata kinetoplast reveals two antipodal sites involved in kinetoplast DNA replication. *Cell* **70**, 612–629.

[13] Kreuzer K N and Cozzarelli N R 1980 Formation and resolution of DNA catenanes by DNA gyrase *Cell* **20**(1) 245–54

[14] Pickett G T 2006, DNA-origami technique for olympic gels *Europhys Lett* **76** 616–22.

[15] Raphaël E, Gay C and de Gennes P G 1997, Progressive Construction of an Olympic gel *J Stat Phys* **89** 111–8.

[16] Rauch, C. A., Perez-Moga, D, Cozzarelli, N. R. and Englund, P. T. (1993) The absence of of supercoiling in kinetoplast DNA minicircles. *EMBO J.* **12**, 403–411.

[17] Shafi KVPM et al 1999, Olympic Ring formation from newly prepared barium hexaferrite nanoparticle suspension *J Phys Chem B* **103**, 3358–60.

[18] Shapiro T and Englund P 1995, The Structure and replication of kinetoplast DNA *Annu Rev Microbiol* **49** 117–43.

[19] Stauffer D and Aharony A 1994, *Introduction to Percolation Theory, Revised Second Edition.* CRC Press, New York, 41-49.

[20] Wikoff W R et al 2000 Topologically linked protein rings in the bacteriophage HK97 capsid *Science* **289**(5487) 2129–33.